Process design analysis of a hybrid Power-and-Biomass-to-Liquid process – An approach combining life cycle and techno-economic assessment

Authors: Julia Weyand[1*], Felix Habermeyer[1], Ralph-Uwe Dietrich[1]

[1]German Aerospace Center (DLR), Institute of Engineering Thermodynamics, Pfaffenwaldring 38-40, 70569 Stuttgart, Germany

*Corresponding author. E-mail address: Julia.Weyand@dlr.de

Abstract

Techno-economically and ecologically optimized processes require understanding of trade-offs between efficiencies, costs and environmental impacts. For this purpose, DLR's in-house tool TEPET for techno-economic analysis was enhanced to enable simultaneous life cycle assessment (LCA). Within this study a hybrid Power-and-Biomass-to-Liquid concept is analysed that can switch between a biomass alone and hydrogen enhanced operation. In order to integrate the techno-economic and ecological results, a dimensionless cost-impact factor is introduced, which gets minimised when both costs and environmental impacts are low. The methodology is applied to investigate process parameter variations within this process concept. The varied process parameters are H_2/CO ratio, H_2 conversion in the Fischer-Tropsch synthesis and CO_2 recycle rate to the gasification. Furthermore, the influence of LCA allocation methods on the preferable set of process parameters was examined. Results show a correlation of lowest environmental impact with high fuel efficiency (energetic fuel output per overall energetic input) for economic allocation. For energetic allocation, high process efficiency (ratio of overall energetic output to overall energetic input) leads to the lowest environmental impact. High carbon efficiency is especially important when biomass has a big impact on a certain category. Sensitivity studies for the global warming potential demonstrate a low sensitivity to the investigated process parameter variations compared with changes in input parameters like biomass and electricity source or transport distance. As the net production cost (NPC) are more sensitive towards the process parameter variations, the cost-impact factor is lowest for the set of process parameters with the lowest NPC.

Keywords: Life Cycle Assessment, Biomass-to-Liquid, Power-and-Biomass-to-Liquid, Techno-Economic Assessment, Fischer-Tropsch, Alternative Fuel

Nomenclature

Abbreviations & Acronyms		Variables	
AEL	Alkaline electrolysis	*CI factor*	Cost-impact factor
AF	Alternative fuel	*i*	Impact category i
ASU	Air separation unit	*NF*	Normalisation factor
BA	Biomass alone	*NR*	Normalised result
BtL	Biomass-to-Liquid	*WF*	Weighting factor
CFB	Circulating fluidised bed	*WR*	Weighted result
CHP	Combined heat and power		
C_{5+}	Hydrocarbons with a chain length of at least five carbon atoms		
EA	Electrolysis assisted		
FF	Fossil fuel		
FLEXCHX	Flexible combined production of power, heat and transport fuels from renewable energy sources		
FT	Fischer-Tropsch		
GHG	Greenhouse gas		
GHSV	Gas hourly space velocity		
GWP	Global warming potential		
HRSG	Heat recovery steam generation system		
LCA	Life cycle assessment		
LCI	Life cycle inventory		
LCIA	Life cycle impact assessment		
LHV	Lower heating value		
NPC	Net production costs		
NTP	Normal temperature and pressure		
PEM	Polymer electrolyte membrane		
PM	Precious metal		
PBtL	Power-and-Biomass-to-Liquid		
PtL	Power-to-Liquid		
RWGS	Reverse water gas shift		
SBCR	Slurry bubble column reactor		
STP	Standard temperature and pressure		
TEA	Techno-economic assessment		
WHSV	Weight hourly space velocity		

1 Introduction

The European Union aims to reduce its greenhouse gas (GHG) emissions by 55 % until 2030 compared with the 1990 levels and become climate neutral by 2050. Fossil fuel use in the transportation sector is a substantial source of GHG emissions, accounting for almost 25 % of the EU's GHG emissions [1]. The energy sector as a whole creates 75% of the EU's GHG emissions [1]. Consequently, expansion of renewable electricity and green fuel production is essential to reach climate neutrality by 2050. The decreased fossil fuel consumption would have the additional benefit of a reduced dependency on oil and gas extracting countries [2]. However, the transition to a predominantly renewable based power system with fluctuating renewable electricity requires a redesign of the energy system where all sectors (electricity, heating, transport, industry) are coupled in combination with storage options [2-4].

The EU project FLEXCHX proposed a process concept that couples the electricity, heating and transport sector to balance out energy system fluctuations. The fuel is produced from biomass via the Fischer-Tropsch (FT) route. Whenever renewable electricity is available, the fuel output can be enhanced with hydrogen from an electrolyser. The off-heat from the process is transformed to district heating and electricity in an adjacent CHP plant [5]. TEA and LCA shall provide information about the technical, economic and ecological feasibility of this process concept. Through identification of bottle-necks, critical process steps as well as cost and environmental impact drivers, TEA and LCA shall furthermore aid the development of an optimised process design.

While several life cycle assessments (LCA) and techno-economic assessments (TEA) for different alternative fuels have been published, no studies consider both in an integrated way [6]. Additionally, multiple studies performing both LCA and TEA have inconsistent system boundaries and functional unit selections, which inhibits the comparison of costs and potential environmental impacts. The integrated approach is further complicated by a lack of consistent methodological guidelines and compatible software tools that allow a simultaneous LCA and TEA with combined result evaluation [6]. However, development and design of optimised processes requires an understanding of trade-offs between cost and environmental impacts, which is not fully available if TEA and LCA are performed separately [7].

The only combined TEA and LCA studies the authors found for alternative fuels via the FT route were limiting the environmental impact analysis to the global warming potential (GWP). AlNouss et al. [8], for example, compared steam and oxygen fed biomass gasification for producing FT liquid, methanol, urea, or power. The GWP only included direct CO_2 emissions and energy consumption for each combination. Overall, steam gasification has the higher net profit and lower global warming potential per kg product for all four products, e.g., 0.7 $\$/kg_{product}$ and 16 $kg_{CO2\text{-}eq.}/kg_{product}$ for FT liquid with steam gasification and -0.8 $/kg$_{product}$ and 64 kg$_{CO2\text{-}eq.}$/kg$_{product}$ for FT liquid with oxygen gasification. Albrecht et al. [9] and Isaacs et al. [10] integrated the economic and ecological results by calculating the greenhouse gas (GHG) abatement cost. Albrecht et al. [9] analysed Power-to-Liquid (PtL) fuel options in Denmark. GHG abatement cost were depicted as a function of fossil fuel reference price, yielding abatement cost in the range of 600 to -350 €$_{2017}$/t$_{CO2\text{-}eq.}$ for fossil fuel reference prices in the range of 0.5 to 3 €/l$_{gasoline}$ (the higher the reference price, the lower the abatement cost). The global warming potential and net production cost were individually calculated to 4.32 g$_{CO2\text{-}eq.}$/MJ$_{fuel}$ and 2.01 €$_{2017}$/l, respectively. Isaacs et al. [10] compared PtL, Biomass-to-Liquid (BtL) and Power-and-Biomass-to-Liquid (PBtL) pathways for the FT synthesis route. Three different biomass sources (corn stover, switchgrass, willow) and four electricity sources (wind, photovoltaic, geothermal and nuclear) were investigated for the US. GHG abatement cost are in the range of 959-1248 $/t$_{CO2\text{-}eq.}$ for PtL, 354-399 $/t$_{CO2\text{-}eq.}$ for BtL and 536-684 $/t$_{CO2\text{-}eq.}$. However, only focussing on GWP/GHG emissions neglects potential trade-offs with other impact categories, where an alternative fuel production process might cause an impact increase compared with fossil fuel.

Since no standardised methodology is available yet for a combined techno-economic and full ecological assessment of alternative fuels, this paper aims to fill this gap. For this purpose, DLR’s in-house software TEPET originally published by Albrecht et al. [11] and further developed by Maier et al. [12] for techno-economic assessment was extended to include an ecological assessment in the form of life cycle assessment (LCA). Process parameters of the FLEXCHX process concept were varied and the effect on multiple impact categories was investigated and then compared with the effect on net production cost. The underlying techno-economic analysis of the process parameter variations was conducted in an already published article by Habermeyer et al. [13]. Additionally, correlations between technical process parameters and environmental impacts as well as ecological trade-offs between the alternative fuel and fossil fuel were examined.

2 Methodology

A simplified illustration of the cost and environmental impact estimation is depicted in Figure 1. Both estimations are based on a detailed process simulation that enables the investigation of different operation conditions (temperature, pressure etc.) and process designs. The simulations are conducted using the commercial AspenPlus® software. When TEPET is linked to such a simulation, equipment dimensions as well as material and energy flows are imported to TEPET and can be automatically updated when process parameters or settings are changed. The simulation inputs are employed to calculate capital and operational expenditures as part of the net production cost (NPC). Further details on the economic calculations can be found in Albrecht et al. [11]. The same material and energy flows are now also utilised as input for the foreground system of the life cycle inventory (LCI). The background system of the LCI is supplied with data from databases like ecoinvent or databases created from literature or project partner data. For the calculation of the life cycle impact assessment (LCIA), the open source LCA software Brightway2 [14] is used.

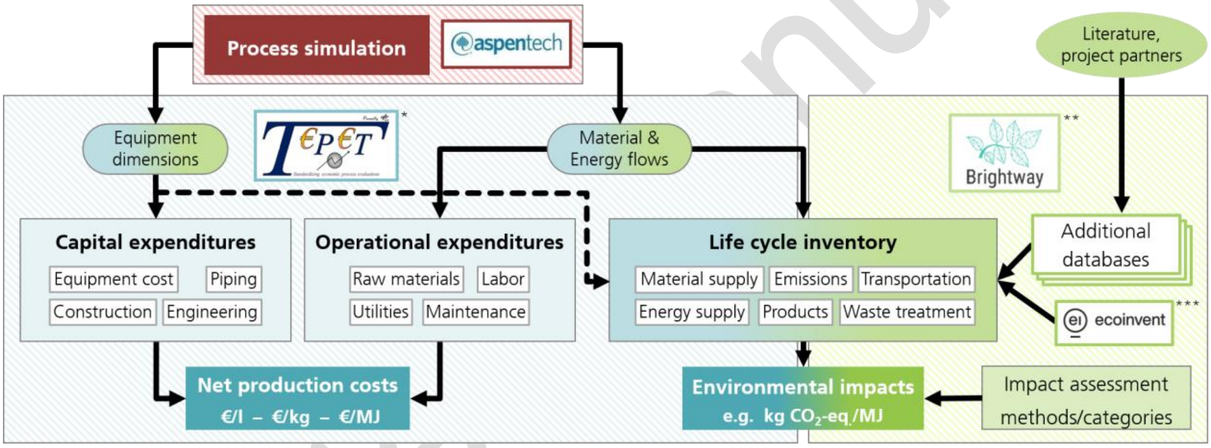

Figure 1: Simplified schematic illustration of cost and environmental impact estimation methodology in TEPET and its Brightway2 extension. * [11, 12], ** [14], * [15].**

2.1 Process concept

The process concept studied in this publication is based on the EU project FLEXCHX [5] with a technology readiness level of 5. The concept consists of two different operation modes: biomass alone (BA, equivalent to BtL) and electrolysis assisted (EA, equivalent to PBtL) [13]. Depending on the availability of renewable electricity the operation mode can be switched on an hourly to daily basis. Additionally, the process off-heat is transferred to a combined heat and power (CHP) plant to generate electricity and district heating [13]. An overview of the two operation modes is shown in Figure 2 and the process flow diagram can be seen in Figure 3.

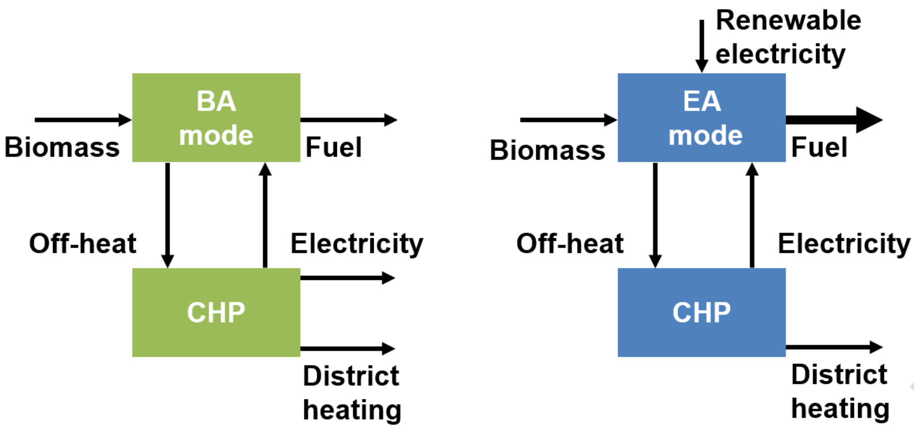

Figure 2: Operation modes of the hybrid process concept. Biomass alone (BA) operation mode (left) and electrolysis assisted (EA) operation mode (right). Adapted from Habermeyer et al. [13].

In a first step, the biomass is dried to reduce the moisture content from 50 $\%_{wt.}$ to 12 $\%_{wt.}$ before entering the circulating fluidised bed (CFB) gasifier. In the gasifier biomass is converted to syngas in the presence of steam and oxygen. Fly ash, which is too light to be removed at the bottom of the gasifier, is removed in a subsequent hot gas filter. As the produced syngas not only contains carbon monoxide and hydrogen but also carbon dioxide, methane, steam, tars, and other traces like ammonia or hydrogen sulphide, auto-thermal tar reforming and gas cleaning steps are necessary. Within the gas cleaning train water and ammonia are removed in a water scrubber, followed by syngas compression, carbon dioxide and hydrogen sulphide removal in a Selexol™ scrubber, and trace removal in a guard bed. The clean syngas then enters the Fischer-Tropsch (FT) synthesis, a slurry bubble column reactor (SBCR), where hydrocarbon chains of different lengths are formed. Chains with a length of five or more (C_{5+}) are separated from the shorter hydrocarbons to be sent to a refinery for transport fuel production. The tail gas (remaining hydrocarbons and unreacted syngas) is partly recycled to the reformer and partly burned to produce heat for the CHP [13].

In the BA mode oxygen is provided by an air separation unit (ASU) and an additional sour shift is needed before the gas cleaning train to adjust the H_2/CO ratio for the FT. In the EA mode oxygen is mainly produced by an alkaline electrolysis (AEL) and only supplemented by oxygen from the ASU if the former does not suffice. The AEL is sized according to the hydrogen demand for adjusting the H_2/CO ratio. Because of the hydrogen addition a partial CO_2 recycle to the gasifier is feasible in the

EA mode to improve the carbon efficiency of the process [13]. The mass ratio of steam and CO_2 to oxygen is fixed to 1.3 for gasification.

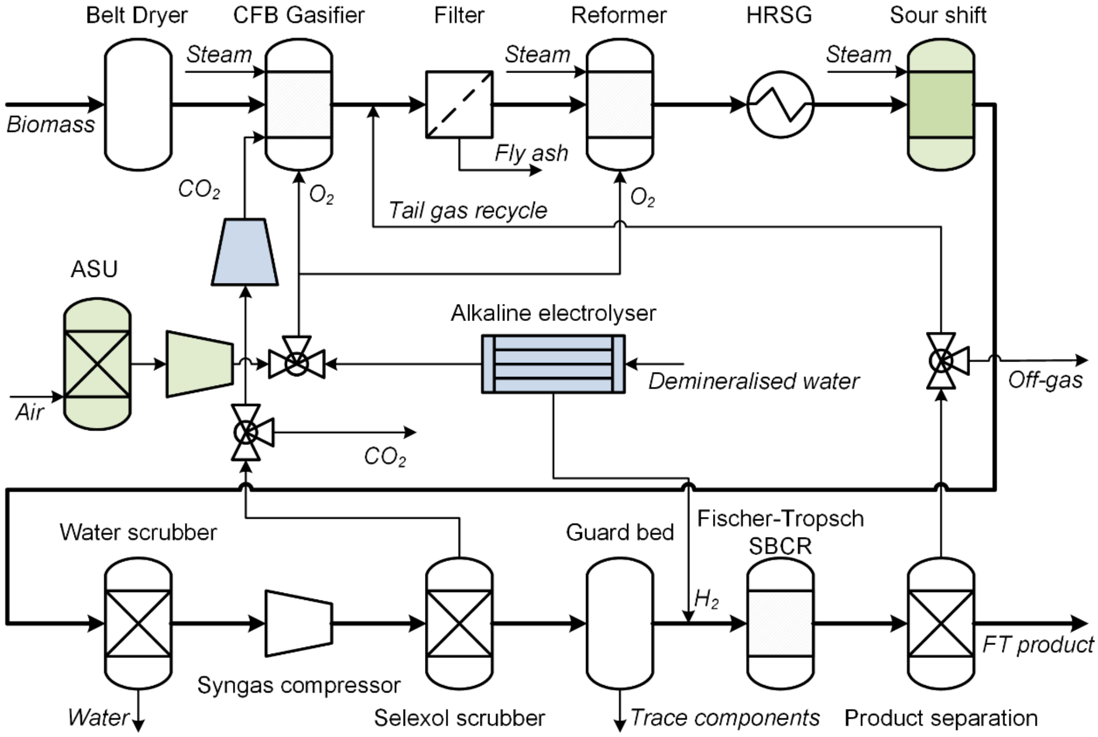

Figure 3: Process flowsheet with BA mode (green, sour shift and ASU) and EA mode (blue, alkaline electrolyser and CO_2 recycle). Adapted from Habermeyer et al. [13].

The considered plant has a capacity of 200 MW_{th} biomass feedstock and is operated for 8100 h/a with a life time of 20 years. The biomass feedstock consists of woody residue chips from forest thinning and industrial wood harvesting [13].

2.2 Process simulation

The process simulation for this work is described in detail in Habermeyer et al. [13]. For the LCA, the calculation of beds, catalysts and solvents was added to the simulation. The required materials and their amounts are listed in Table 1.

The sand and dolomite bed mixture is used in the gasifier to maintain stable fluidisation and to catalyse tar decomposition [16]. In the reformer ZrO_2 catalyst selectively oxidises heavy tars followed by further hydrocarbon decomposition in the precious metal (PM) catalyst layer in order to enable methane reforming in the Ni catalyst layer without issues from coking or soot [17]. Sulphur-tolerant

Co/Mo catalyst catalyses the water-gas shift reaction in the sour-shift [17] while Selexol™ serves as a solvent for carbon dioxide (90 %) and hydrogen sulphide (99 %) removal [18]. Residual sulphur amounts are eventually removed with the ZnO guard bed to avoid poisoning of the Co/Re Fischer-Tropsch synthesis catalyst [17].

Table 1: Additional materials (beds, catalysts, solvents) and their amounts.

Materials	Lifetime [a]	Amount	Unit	Additional information	Unit
Sand/dolomite	-	0.06 [16, 19]	$kg/kg_{biomass}$	30 $\%_{wt.}$ silica sand & 70 $\%_{wt.}$ dolomite [16]	A
ZrO_2 catalyst [b]	2 [a] [20]	0.2 [21]	10^{-3} m^3/m^3_{syngas}*h [c]	50 $\%_{wt.}$ ZrO_2 on Al_2O_3 [21]	B
Precious metal (PM) catalyst [b]	2 [a] [20]	0.07 [21]	10^{-3} m^3/m^3_{syngas}*h [c]	1.5 $\%_{wt.}$ PM on Al_2O_3 [21], PM=Rh [22-24]	B
Ni catalyst [b]	2 [a] [20]	0.2 [21]	10^{-3} m^3/m^3_{syngas}*h [c]	15 $\%_{wt}$ Ni on Al_2O_3 [25-27]	B
Co/Mo catalyst [b]	3 [a] [28]	0.25 [29, 30]	10^{-3} m^3/m^3_{syngas}*h [d]	5 $\%_{wt}$ CoO, 15 $\%_{wt}$ MoO_3 on 60 $\%_{wt}$ Al_2O_3 and 20 $\%_{wt}$ MgO [30]	C
Selexol™	-	0.007 [31]	kg/t_{CO2}		D
ZnO	-	5	kg/kg_S	Assumption: 50 % of max. adsorption capacity [32]	E
Co/Re catalyst	3 [a] [33]	calculated in [13]	kg/h	25 $\%_{wt.}$ Co and 0.48 $\%_{wt.}$ Re on Al_2O_3 [34]	F

A: Gasifier, B: Reformer, C: Sour shift, D: Selexol™ scrubber, E: Guard bed, F: Fischer-Tropsch

[a] Full load hours: 8100 h/a [13]

[b] catalyst bulk density (assumed for catalyst with Al_2O_3 support based on Vega-Merino et al. [35], BASF [36], Griffiths et al. [37], Suehiro et al. [38]): 800 kg/m^3

[c] space velocity assumed to be gas hourly space velocity (GHSV) because of the order of magnitude of the numerical values and the normal temperature and pressure (NTP) specification even though weight hourly space velocity (WHSV) is written in the patent [21]

[d] Standard temperature and pressure (STP) is assumed for GHSV as the typical condition according to Bartholomew et al. [39]

2.3 Case studies

Within this study three process parameter variations are investigated:

- H_2/CO ratio
- H_2 conversion in the FT synthesis

- CO_2 recycle rate to adjust steam replacement in the gasification

Table 2 summarises the key findings of the techno-economic assessment done by Habermeyer et al. [13] for the three process parameter variations. The cases with a variation in the CO_2 recycle rate (1.5 and 1.6) were recalculated for this work since they were not part of the original publication by Habermeyer et al. [13]. The recalculation is based on the same approach and assumptions of the original publication [13] and replaced the variation in biomass feed rate in EA mode (cases 2.1 to 2.4). The lower biomass feed rate in the EA mode studied in Habermeyer et al. [13] reduces the capacity of the electrolyser which has an economic effect but the effect on the environment is negligible, as can be seen in the results section.

The higher H_2/CO ratio of 2.05 corresponds to the stoichiometric consumption [18]. While the ratio of 2.05 provides a higher product yield, the lower ratio of 1.6 has the advantage of a higher C_{5+} selectivity [40]. Additionally, a lower H_2/CO ratio results in a higher carbon efficiency for the BA mode because less CO is converted to CO_2 in the water gas shift reactor to reach the H_2/CO ratio [13]. For the EA mode a lower ratio entails a lower electricity demand for the electrolyser as less hydrogen needs to be produced [13].

The H_2 conversion affects the product yield and C_{5+} selectivity as well. Higher H_2 conversions naturally achieve a higher product yield while simultaneously improving the C_{5+} selectivity due to higher steam to hydrogen ratios. Water is known to enhances chain propagation even though the mechanistic explanation is not clear yet [41]. However, if the steam to hydrogen ratio gets too high, which happens for lower H_2/CO ratios at lower H_2 conversion rates, damages to the catalyst can occur [41]. High partial pressures of water can deactivate the catalyst by causing re-oxidation of the cobalt metal [42]. Thus, a lower and a higher H_2 conversion of 55 % and 70 % are examined for both H_2/CO ratios [13].

The CO_2 recycle rate in the EA mode is only varied for the higher H_2/CO of 2.05 and higher H_2 conversion of 70 % (equivalent to case 1.1). The CO_2 recycle rate is increased from around 30 % to 40 % and then 80 %. The latter value corresponds to a maximum steam replacement of 100 % in the gasifier. On the one hand, a higher CO_2 recycle rate increases the carbon efficiency, but on the other, it also increases the electricity requirement. The additional electricity is primarily needed to meet the enhanced hydrogen demand for a carbon richer syngas and partially to compress the larger recycle stream.

Table 2: Key process simulation, efficiency and economic results [13]. Highest efficiencies and lowest costs per mode are bold.

Case	1.1	1.2	1.3	1.4	1.5	1.6
H_2/CO [-]	2.05	2.05	1.6	1.6	2.05	2.05
H_2 conversion [%]	70	55	70	55	70	70
Steam replacement with recycled CO_2 – EA [%]	65	65	65	65	80	100
CO_2 recycle rate – EA [%]	32.6	33.0	30.0	30.0	40.2	80.0
Biomass feed rate BA/EA [MW_{th}]	200	200	200	200	200	200
BA						
FT-product output [kg/s]	2.62	2.53	2.66	2.56	2.62	2.62
FT-product LHV [MJ/kg]	43.9	43.9	43.8	43.8	43.9	43.9
District heating output [MW_{th}]	37.5	42.3	37.1	42.6	37.5	37.5
Electricity output [MW_{el}]	2.1	3.4	1.8	3.3	2.1	2.1
Fuel Efficiency [%]	57.6	55.6	**58.4**	56.0	57.6	57.6
Process Efficiency [%]	77.4	78.5	77.8	**79.0**	77.4	77.4
Carbon Efficiency [%]	35.4	34.2	**35.9**	34.5	35.4	35.4
FT-product NPC [€$_{2019}$/l]	1.08	1.13	**0.98**	1.03	1.15	1.41
FT-product NPC [€$_{2019}$/MJ] [a]	0.034	0.035	**0.031**	0.032	0.036	0.044
EA						
FT-product output [kg/s]	4.53	4.48	4.15	4.04	4.81	5.8
FT-product LHV [MJ/kg]	43.9	43.9	43.8	43.9	43.9	43.9
District heating output [MW_{th}]	66.2	76.3	59.3	69.0	70.4	93.9
Electricity input AEL [MW_{el}]	187.9	198.7	145.2	151.8	214.6	332.9
Electricity input total [MW_{el}]	160.2	167.2	124.0	127.2	183.6	289.8
CO_2 recycle [%]	32.6	33.0	30.0	30.0	40.2	80
Fuel Efficiency [%]	55.2	53.6	**56.1**	**54.2**	55.0	52.0
Process Efficiency [%]	73.6	74.3	74.4	75.3	73.4	71.2
Carbon Efficiency [%]	61.1	60.4	56.0	54.5	64.8	**78.2**
FT-product NPC [€$_{2019}$/l]	1.04	1.07	**0.98**	1.01	1.07	1.21
FT-product NPC [€$_{2019}$/MJ] [a]	0.032	0.033	**0.031**	0.032	0.033	0.038

[a] 0.729 kg/l [11] and FT-product LHV of individual case

2.4 Life cycle assessment

The functional unit for the LCA is 1 MJ (LHV) of produced Fischer-Tropsch (FT) product and the production facility is assumed to be located in Finland. The LCI is divided into several subsystems which correlate with the units of the production process described in 2.1 and additional subsystems for the biomass supply, transportation, plant construction as well as product upgrading and combustion. Electricity and heat are only considered as the total flows illustrated in Figure 2 when exiting or entering the plant. Table 3 and Table 4 depict the aggregated inventory data of the foreground system for the 6 cases in BA and EA mode, respectively. The unaggregated inventory version with the subsystem mentioned prior is attached in the Supplementary Information (SI Table 2). The secondary inventory data of the background system and their ecoinvent 3.8 (Allocation, cut-off by classification) [15] dataset connections can be found in the Supplementary Information as well (SI Tables 3-21). The LCA follows the attributional approach from well to wheel.

Woody residues are considered to be a mixture of bark chips from debarking in forest and wood chips from sustainable forestry management. The amounts were calculated based on the three dominating tree species in Finland, their average bark proportion and the percentage of chips generated during harvesting. The tree species found in Finland are predominantly pine (49.8 $\%_{vol.}$) and spruce (30.2 $\%_{vol.}$), followed by birch (16.7 $\%_{vol.}$) [43]. Their wood densities range between 370-550 kg/m^3, 300-470 kg/m^3 and 590-740 kg/m^3 for pine, spruce and birch, respectively [44]. The average proportions of bark for these three species were calculated based on the mean bark proportions at relative heights of 10-90 % as listed in Liepiņš et al. [45], yielding 11.0 $\%_{vol.}$ bark for pine, 13.8 $\%_{vol.}$ for spruce and 12.9 $\%_{vol.}$ for birch. Similar proportions can be found in Routa et al. [46] with 10-15 $\%_{wt.}$ bark and Nosek et al. [47] with 5-15 % bark for softwood and 5-20 % for hardwood. Here, volume and mass basis are considered as interchangeable because the same density was assumed for bark and wood under bark. According to the ecoinvent 3.8 [48] documentation for wood chips in Sweden harvesting generates 5.616 $\%_{vol}$ wood chips per m^3 solid wood under bark for pine and spruce and 37.44 $\%_{vol}$ for birch. Since the woody residues have an economic value in Habermeyer et al. [13], they are not regarded as waste and therefore carry an environmental burden.

Ash, removed at the bottom of the gasifier and in the subsequent filter, is sent to a sanitary landfill. For the catalyst production, only the chemical inputs were considered due to a lack of more detailed information. The catalyst compositions are stated in Table 1 and some further assumptions are described below. The chosen precious metal (PM), rhodium, of the PM catalyst in the reformer is estimated to be 90 % recyclable [49, 50], which is modelled by a slightly adjusted automobile catalyst recycling process. As reported by Santos et al. [25], Ni catalyst (reformer) can be produced by incipient wetness, using $Ni(NO_3)_2{\cdot}H_2O$ as a precursor. As $Ni(NO_3)_2{\cdot}6H_2O$ contains 20.18 $\%_{wt.}$ Ni, at least 0.7433 kg nickel nitrate are needed for 1 kg of catalyst with 15 $\%_{wt.}$ Ni on Al_2O_3 support. Nickel nitrate is produced by the following chemical reaction [51]:

$$NiO + 2\ HNO_3 + 5\ H_2O \rightarrow Ni(NO_3)_2 \cdot 6H_2O \quad \mathbf{(2.1)}$$

The Co/Re catalyst for the FT synthesis is prepared by slurry impregnation with $Co(H_2O)_6(NO_3)_2$ and aqueous incipient wetness impregnation with Re_2O_7 [34]. The following reaction was chosen for the production of cobalt nitrate [51]:

$$CoO + 2\ HNO_3 + 5\ H_2O \rightarrow Co(H_2O)_6(NO_3)_2 \quad \mathbf{(2.2)}$$

Selexol™, dimethyl ethers of polyethylene glycol ($CH_3O[CH_2CH_2O]_nCH_3$), is deduced to be created from ethylene oxide and methanol according to the following reactions:

$$C_2H_4O + H_2O \rightarrow HOCH_2CH_2OH \quad \mathbf{(2.3)}$$

$$HOCH_2CH_2OH + (n\text{-}1)\ C_2H_4O \rightarrow HO[CH_2CH_2O]_nH \quad \mathbf{(2.4)}$$

$$HO[CH_2CH_2O]_nH + 2\ CH_3OH \rightarrow CH_3O[CH_2CH_2O]_nCH_3 + 2\ H_2O \quad \mathbf{(2.5)}$$

where n is in the range of 2 to 12 [52-55] with a median value of 6. The median value is used to calculate the amounts of chemicals needed for 1 kg of Selexol™. Additionally, data for water, natural gas, steam and electricity consumption as well as emissions could be obtained from Schakel et al. [56]. All spent catalysts as well as the spent ZnO bed are assumed to be sent to a hazardous waste landfill while spent Selexol™ is discarded in a hazardous waste incineration [57]. Only sand and dolomite from the gasifier bed are sent to an inert waste landfill [57]. Treatment of the wastewater from the water scrubber and FT-product separation train is approximated by an average wastewater treatment plant operation.

The electricity consumed in the EA mode is assumed to be generated by onshore wind turbines in Finland. The fuel synthesis plant construction is modelled according to Jungbluth et al. [58], which has a capacity of $2.02 \cdot 10^8$ kg/a, a life time of 20 a and an operation time of 8000 h/a. The ASU and CHP both have a lifetime of 20 a and are scaled based on appropriate ecoinvent datasets. The AEL construction is based on a 6 MW cell stack by Koj et al. [59], who also provides information about the electrolyte composition and consumption. The electrolyte is a 25 $\%_{wt.}$ KOH solution that requires 10 kg deionised water and 1.9 g potassium hydroxide per kg hydrogen produced [59]. The larger unit of both modes is adopted for the plant construction in BA and EA mode. The originally calculated units for each mode can be found in the Supplementary Information (SI Table 2).

Biomass is estimated to be transported for 100 km [60-62] with a 40 t truck [61], while the FT-product is assumed to be transported for around 200 km to a nearby refinery with a 16-32 t truck (own estimation). The green FT- diesel is assumed to be produced at an ordinary European petroleum refinery with an efficiency of 93.5% [63], which means that 1.07 $MJ_{FT\text{-}product}$ corresponds to 1 $MJ_{green\ FT\text{-}diesel}$ (1 $kg_{FT\text{-}product} \triangleq 0.96\ kg_{green\ FT\text{-}diesel}$ with $LHV_{FT\text{-}product}$ from Table 2 and $LHV_{green\ FT\text{-}diesel}$ = 42.6 MJ/kg [64]). The green FT-diesel distribution is considered analogue to fossil diesel distribution. However, the pipeline transport included in the fossil diesel dataset is reduced for the FT-diesel distribution to exclude import to Europe [65]. The combustion of green FT-diesel is estimated with diesel combustion in a diesel engine of a EURO 5 medium size passenger car. The sulphur dioxide emissions are neglected due to a high reduction and therefore low sulphur concentration of 0.005 ppm before the FT synthesis [17]. Nitrogen oxides, particulate matter, carbon monoxide and hydrocarbons combustion emissions are reduced by 29 %, 94 %, 92 % and 72 %, respectively, based on Lappas et al. [66] compared with fossil diesel combustion. For the comparison with fossil fuel, combustion of fossil diesel is assumed to take place in the same diesel engine of a EURO 5 medium size passenger car.

Table 3: Life cycle inventory of the foreground system for BA mode.

Exchange	Type	Unit	Case 1.1	1.2	1.3	1.4	1.5	1.6
BA								
Woody residues	Input	kg	23.68	23.68	23.68	23.68	23.68	23.68
Gasifier bed	In- / Output	kg	0.80	0.80	0.80	0.80	0.80	0.80
ZrO_2 catalyst	In- / Output	kg	$4.1\cdot10^{-4}$	$4.6\cdot10^{-4}$	$4.2\cdot10^{-4}$	$4.8\cdot10^{-4}$	$4.1\cdot10^{-4}$	$4.1\cdot10^{-4}$
PM catalyst	In- / Output	kg	$1.4\cdot10^{-4}$	$1.6\cdot10^{-4}$	$1.4\cdot10^{-4}$	$1.6\cdot10^{-4}$	$1.4\cdot10^{-4}$	$1.4\cdot10^{-4}$
Ni catalyst	In-/ Output	kg	$4.1\cdot10^{-4}$	$4.6\cdot10^{-4}$	$4.2\cdot10^{-4}$	$4.8\cdot10^{-4}$	$4.1\cdot10^{-4}$	$4.1\cdot10^{-4}$
Co/Mo catalyst	In- / Output	kg	$9.9\cdot10^{-5}$	$1.0\cdot10^{-4}$	$5.7\cdot10^{-5}$	$5.6\cdot10^{-5}$	$9.9\cdot10^{-5}$	$9.9\cdot10^{-5}$
Selexol™	In- / Output	kg	$1.1\cdot10^{-4}$	$1.1\cdot10^{-4}$	$1.1\cdot10^{-4}$	$1.1\cdot10^{-4}$	$1.1\cdot10^{-4}$	$1.1\cdot10^{-4}$

ZnO	In- / Output	kg	$7.0\cdot10^{-4}$	$7.0\cdot10^{-4}$	$7.0\cdot10^{-4}$	$7.0\cdot10^{-4}$	$7.0\cdot10^{-4}$	$7.0\cdot10^{-4}$
Co/Re catalyst	In- / Output	kg	$2.7\cdot10^{-4}$	$1.8\cdot10^{-4}$	$2.8\cdot10^{-4}$	$1.9\cdot10^{-4}$	$2.7\cdot10^{-4}$	$2.7\cdot10^{-4}$
Plant construction								
Fuel synthesis plant	Input	unit	$1.1\cdot10^{-9}$	$1.1\cdot10^{-9}$	$1.0\cdot10^{-9}$	$1.0\cdot10^{-9}$	$1.2\cdot10^{-9}$	$1.4\cdot10^{-9}$
AEL electrolysis stack	Input	unit	$5.4\cdot10^{-8}$	$5.7\cdot10^{-8}$	$4.2\cdot10^{-8}$	$4.3\cdot10^{-8}$	$6.1\cdot10^{-8}$	$9.5\cdot10^{-8}$
Air separation unit	Input	unit	$2.1\cdot10^{-8}$	$2.1\cdot10^{-8}$	$2.1\cdot10^{-8}$	$2.1\cdot10^{-8}$	$2.1\cdot10^{-8}$	$2.1\cdot10^{-8}$
CHP plant	Input	unit	$1.8\cdot10^{-8}$	$2.0\cdot10^{-8}$	$1.6\cdot10^{-8}$	$1.8\cdot10^{-8}$	$1.9\cdot10^{-8}$	$2.5\cdot10^{-8}$
Transport								
Biomass transport	Input	t*km	2.37	2.37	2.37	2.37	2.37	2.37
FT-product transport	Input	t*km	0.52	0.51	0.53	0.51	0.52	0.52
Wastes								
Ash	Output	kg	0.59	0.59	0.59	0.59	0.59	0.59
Removed traces	Output	kg	$2.9\cdot10^{-4}$	$2.9\cdot10^{-4}$	$2.9\cdot10^{-4}$	$2.9\cdot10^{-4}$	$2.9\cdot10^{-4}$	$2.9\cdot10^{-4}$
Wastewater	Output	m^3	0.01	0.01	0.01	0.01	0.01	0.01
Product upgrading & combustion								
Refinery operation	Input	kg	-2.52	-2.44	-2.56	-2.46	-2.52	-2.52
FT-diesel distribution	Input	kg	-2.52	-2.44	-2.56	-2.46	-2.52	-2.52
FT-diesel combustion	Input	kg	-2.52	-2.44	-2.56	-2.46	-2.52	-2.52
Products								
FT-product	Output	kg	2.62	2.53	2.66	2.56	2.62	2.62
District heating (CHP)	Output	MJ	37.53	42.3	37.12	42.63	37.53	37.53
Electricity (CHP)	Output	kWh	0.59	0.93	0.49	0.91	0.59	0.59
Environment								
Air (N_2)	Input	kg	509.04	510.15	508.61	509.95	509.04	509.04
Air (O_2)	Input	kg	154.56	154.91	154.43	154.84	154.56	154.56
Water	Input	m^3	0.01	0.01	0.01	0.01	0.01	0.01
Off-gas (N_2)	Output	kg	509.06	510.18	508.64	509.97	509.06	509.06
Off-gas (O_2)	Output	kg	146.49	146.52	146.49	146.53	146.49	146.49
Off-gas (H_2O)	Output	m^3	0.01	0.01	0.01	0.01	0.01	0.01
Off-gas (CO_2)	Output	kg	14.37	14.65	14.24	14.58	14.37	14.37
Off-gas (H_2S)	Output	kg	$4.9\cdot10^{-3}$	$4.9\cdot10^{-3}$	$4.9\cdot10^{-3}$	$4.9\cdot10^{-3}$	$4.9\cdot10^{-3}$	$4.9\cdot10^{-3}$

Table 4: Life cycle inventory of the foreground system for EA mode.

Exchange	Type	Unit	Case					
			1.1	1.2	1.3	1.4	1.5	1.6
EA								
Woody residues	Input	kg	23.68	23.68	23.68	23.68	23.68	23.68
Gasifier bed	Input	kg	0.80	0.80	0.80	0.80	0.80	0.80
ZrO_2 catalyst	In- / Output	kg	$4.5\cdot10^{-4}$	$5.5\cdot10^{-4}$	$4.5\cdot10^{-4}$	$5.5\cdot10^{-4}$	$4.5\cdot10^{-4}$	$5.3\cdot10^{-4}$
PM catalyst	In- / Output	kg	$1.5\cdot10^{-4}$	$1.8\cdot10^{-4}$	$1.5\cdot10^{-4}$	$1.8\cdot10^{-4}$	$1.5\cdot10^{-4}$	$1.8\cdot10^{-4}$
Ni catalyst	In- / Output	kg	$4.5\cdot10^{-4}$	$5.5\cdot10^{-4}$	$4.5\cdot10^{-4}$	$5.5\cdot10^{-4}$	$4.5\cdot10^{-4}$	$5.3\cdot10^{-4}$
Selexol™	In- / Output	kg	$9.0\cdot10^{-5}$	$8.8\cdot10^{-5}$	$9.7\cdot10^{-5}$	$9.7\cdot10^{-5}$	$8.9\cdot10^{-5}$	$1.4\cdot10^{-4}$

ZnO	In- / Output	kg	$7.0\cdot10^{-4}$	$7.0\cdot10^{-4}$	$7.0\cdot10^{-4}$	$7.0\cdot10^{-4}$	$7.0\cdot10^{-4}$	$7.0\cdot10^{-4}$
Co/Re catalyst	In- / Output	kg	$4.2\cdot10^{-4}$	$3.0\cdot10^{-4}$	$4.0\cdot10^{-4}$	$2.8\cdot10^{-4}$	$4.4\cdot10^{-4}$	$5.4\cdot10^{-4}$
AEL electrolyte	Input	kg	8.39	8.87	6.48	6.78	9.58	14.86
Wind electricity	Input	kWh	44.50	46.44	34.45	35.33	51.00	80.49
Plant construction								
Fuel synthesis plant	Input	unit	$1.1\cdot10^{-9}$	$1.1\cdot10^{-9}$	$1.0\cdot10^{-9}$	$1.0\cdot10^{-9}$	$1.2\cdot10^{-9}$	$1.4\cdot10^{-9}$
AEL electrolysis stack	Input	unit	$5.4\cdot10^{-8}$	$5.7\cdot10^{-8}$	$4.2\cdot10^{-8}$	$4.3\cdot10^{-8}$	$6.1\cdot10^{-8}$	$9.5\cdot10^{-8}$
Air separation unit	Input	unit	$2.1\cdot10^{-8}$	$2.1\cdot10^{-8}$	$2.1\cdot10^{-8}$	$2.1\cdot10^{-8}$	$2.1\cdot10^{-8}$	$2.1\cdot10^{-8}$
CHP plant	Input	unit	$1.8\cdot10^{-8}$	$2.0\cdot10^{-8}$	$1.6\cdot10^{-8}$	$1.8\cdot10^{-8}$	$1.9\cdot10^{-8}$	$2.5\cdot10^{-8}$
Transport								
Biomass transport	Input	t*km	2.37	2.37	2.37	2.37	2.37	2.37
FT-product transport	Input	t*km	0.91	0.90	0.83	0.81	0.96	1.16
Wastes								
Ash	Output	kg	0.59	0.59	0.59	0.59	0.59	0.59
Removed traces	Output	kg	$2.9\cdot10^{-4}$	$2.9\cdot10^{-4}$	$2.9\cdot10^{-4}$	$2.9\cdot10^{-4}$	$2.9\cdot10^{-4}$	$2.9\cdot10^{-4}$
Wastewater	Output	m^3	0.01	0.02	0.01	0.01	0.01	0.02
Product upgrading & combustion								
Refinery operation	Input	kg	-4.36	-4.31	-3.99	-3.89	-4.63	-5.59
FT-diesel distribution	Input	kg	-4.36	-4.31	-3.99	-3.89	-4.63	-5.59
FT-diesel combustion	Input	kg	-4.36	-4.31	-3.99	-3.89	-4.63	-5.59
Products								
FT-product	Output	kg	4.53	4.48	4.15	4.04	4.81	5.80
District heating (CHP)	Output	MJ	66.17	76.31	59.28	69.02	70.43	93.85
Environment								
Air (N_2)	Input	kg	487.48	488.26	491.86	493.24	485.03	485.57
Air (O_2)	Input	kg	148.02	148.25	149.35	149.76	147.27	147.44
Water	Input	m^3	$5.8\cdot10^{-3}$	$6.0\cdot10^{-3}$	$5.5\cdot10^{-3}$	$5.7\cdot10^{-3}$	$5.9\cdot10^{-3}$	$6.5\cdot10^{-3}$
Off-gas (N_2)	Output	kg	487.51	488.29	491.88	493.27	485.05	485.6
Off-gas (O_2)	Output	kg	146.54	146.61	146.53	146.6	146.55	146.57
Off-gas (H_2O)	Output	m^3	0.01	0.01	0.01	0.01	0.01	0.01
Off-gas (CO_2)	Output	kg	8.43	8.59	9.62	9.95	7.56	4.48
Off-gas (H_2S)	Output	kg	$4.9\cdot10^{-3}$	$4.9\cdot10^{-3}$	$4.9\cdot10^{-3}$	$4.9\cdot10^{-3}$	$4.9\cdot10^{-3}$	$4.9\cdot10^{-3}$

For the life cycle impact assessment (LCIA) the Environmental Footprint method *EF v3.0 no LT* was chosen [67] because it was developed by the European Commission for the European context and is one of the newest methods. Furthermore, standardised normalisation and weighting factors are available for this method, which are necessary for the combined TEA and LCA evaluation in this publication.

Since the assessed process is a multi-output process, allocation is performed. Allocation is the partitioning of environmental impacts between different products (here: FT-product, district heating, electricity) according to their physical (mass, energy, exergy), economic or causal contribution to the overall product output. Both energetic and economic allocation will be investigated in this publication as both are reasonable criteria for this process and there is no societal preference whether environmental impacts should be minimised towards economic value creation/competitiveness or conversion maxima (from biomass and power to fuel and by-products). The product outputs as well as the heating value of the FT-product for the energetic allocation can be found in Table 2. The selling prices used to calculate the economic allocation factors are listed in Table 5. The computed energetic and economic allocation factors for the FT-product are summarised in

Table 6. The difference to 1 is allocated towards district heating in EA mode or district heating and electricity in BA mode. Overall, allocation factors are higher for economic than energetic allocation because the monetary value is higher than the energy content in the FT-product compared to the other products.

Table 5: Product selling prices.

Product	Price	Source
FT-product	Case specific NPCs in Table 2 (112 – 158 €/MWh_{LHV})	[13]
District heating	40 €/MWh_{th}	[17]
Electricity	50.4 €/MWh_{el}	[17]

Table 6: FT-product allocation factors.

Allocation method	Case 1.1	1.2	1.3	1.4	1.5	1.6
BA						
energetic	0.744	0.709	0.750	0.709	0.744	0.744
economic	0.897	0.884	0.891	0.874	0.897	0.897
EA						
energetic	0.750	0.720	0.754	0.720	0.750	0.731
economic	0.898	0.886	0.894	0.880	0.896	0.888

2.5 Combined TEA and LCA evaluation

In order to understand the relationship between economic efforts and environmental benefit, TEA and LCA have to be combined, for which the cost impact factor is introduced. In a first step, normalisation is performed on the LCIA results of all 16 impact categories from the Environmental Footprint method to establish comparability. The normalised results (*NR*) are calculated according to the following equation:

$$NR_i = \frac{LCIA\ result_i}{NF_i} \qquad \textbf{(2.6)}$$

where *i* represents an impact category and *NF* the respective normalisation factor taken from European Commission [68].

Next, the normalised results are weighted to receive one impact score, the weighted result (*WR*):

$$WR = \sum_{i=1}^{16} WF_i * NR_i \qquad \textbf{(2.7)}$$

where *i* is an impact category and *WF* the associated weighing factor from Sala et al. [69].

The weighted result of all environmental impacts is then used to calculate the dimensionless cost-impact factor (*CI factor*) by multiplying the weighted (impact) result with the net production cost (*NPC*) of alternative fuel (*AF*) relative to fossil fuel (FF):

$$CI\ factor = \frac{WR_{AF}}{WR_{FF}} * \frac{NPC_{AF}}{NPC_{FF}} \qquad \textbf{(2.8)}$$

WR_{FF} for fossil diesel is calculated to be $8.56 \cdot 10^{-16}$ MJ^{-1}. Since the FT-product still needs to be refined, the crude oil price is chosen as the fossil fuel comparator with 0.48 $€_{2019}$/l [70, 71] and 36.1 MJ/l [72]. Refining is included in both *NPC* with 0.036 $€_{2019}$/l [71, 73] and an energetic efficiency of 93.5 % for diesel production [63].

Simultaneously, another approach was considered where the focus of the combined evaluation lies on the cost for avoided greenhouse gas (*GHG*) emissions of the alternative fuel (*AF*) compared to fossil fuel (*FF*):

$$GHG\ abatement\ cost = \frac{NPC_{AF} - NPC_{FF}}{GWP_{FF} - GWP_{AF}} \qquad \textbf{(2.9)}$$

where *GWP* stands for global warming potential. The fossil fuel reference value (94 $g_{CO2\text{-}eq.}$/MJ) of the Renewable Energy Directive (RED) was selected for GWP_{FF} [74].

3 Results and Discussion

This section presents the results of the LCA for two different operation modes and the influence of varying process parameters on the ecological assessment. Furthermore, the effect of different allocation methods on the preferable process parameter variant is shown. The outcomes are compared with the techno-economic results investigated by Habermeyer et al. [13].

3.1 Environmental impact contributions

A majority of the global warming potential (GWP) in the BA mode (Figure 4) stems from the biomass harvesting (~40 $\%_{BA}$) and its transport to the facility (~19 $\%_{BA}$). Harvesting includes various machinery operated with fossil diesel and transport is carried out with diesel trucks. The total GWP in case 1.4 amounts to 7.5 $g_{CO2\text{-}eq.}/MJ_{green\ FT\text{-}diesel}$ with energetic or 9.2 $g_{CO2\text{-}eq.}/MJ_{green\ FT\text{-}diesel}$ with economic allocation, which is equivalent to 8 % and 10 % of GWP_{FF}, respectively. REDII requires a 65 % GWP reduction of biofuels produced in new installations (operation started after 2021) compared with fossil fuels ($GWP_{AF} \leq 35$ % of GWP_{FF}). In the EA mode (Figure 5) impact from wind energy is added while the total impact from biomass and its transport is simultaneously reduced because of an increased carbon conversion. Around 48 % of GWP from wind energy derives from steel, 10 % from glass fibre and 8 % from concrete. Relatively, wind energy, biomass, and transport contribute with ~33 $\%_{EA}$, ~23 $\%_{EA}$, and ~11 $\%_{EA}$ to the total GWP of case 1.4 (energetic alloc.: 8.5 $g_{CO2\text{-}eq.}/MJ_{green\ FT\text{-}diesel} \triangleq 9$ % of GWP_{FF}, economic alloc.: 10.4 $g_{CO2\text{-}eq.}/MJ_{green\ FT\text{-}diesel} \triangleq 11$ % of GWP_{FF}). In both modes the next biggest impacts are attributed to the fuel synthesis plant construction (~10 $\%_{BA}$, ~9 $\%_{EA}$), FT-product transport (~8 $\%_{BA}$, ~7 $\%_{EA}$), green FT-diesel distribution (~5 $\%_{BA}$, ~4 $\%_{EA}$), gasifier bed material production (~5 $\%_{BA}$, ~3 $\%_{EA}$) and green FT-diesel combustion (~3 $\%_{BA}$, ~3 $\%_{EA}$).

Biomass harvesting and electricity generation have a significant influence on almost all of the 16 impact categories due to the comparatively high consumption in the process. Other important factors are the green FT-diesel combustion emissions, transport, fuel synthesis plant construction and direct emissions. The direct emission impact (light blue) of freshwater ecotoxicity originates from the hydrogen sulphide removed with the Selexol™ scrubber while the direct emissions impact of water use predominantly stems from the water vapor released during woody biomass drying (59 $\%_{BA}$ and

41 $\%_{EA}$ direct emissions of water use equals 0.10 and 0.07 $kg_{H_2O}/MJ_{green\ FT\text{-}diesel}$, respectively). The impact from fuel synthesis plant construction is attributed to electricity, electronics and various metals (mainly steel, aluminium, copper, and solder) in varying proportions (e.g., GWP: 25 % European grid mix electricity, 25 % steel, 16 % electronics, 7 % aluminium, and 3 % copper). Transport causes environmental impacts through road construction, diesel and lorry production for all categories as well as additional combustion emissions, tyre wear, brake wear and road wear for some categories (e.g., GWP: 69 % combustion emissions, 16 % road construction and 12 % diesel production, 2 % lorry production). FT-diesel combustion impact is primarily driven by nitrogen oxides emissions for a multitude of categories: particulate matter, photochemical ozone formation, acidification, terrestrial eutrophication, marine eutrophication. Global warming potential, human toxicity with cancer effects and human toxicity with non-cancer effects on the other hand are affected by dinitrogen oxide, formaldehyde and acrolein emissions from FT-diesel combustion, respectively.

Interestingly, the gasifier bed material and the precious metal reformer catalyst have a significant contribution to some impact categories (e.g., global warming, ionising radiation, freshwater ecotoxicity and resource use of fossils as well as minerals and metals) even though only small quantities are required for the process. The gasifier bed material impact (e.g., ionising radiation: 9 $\%_{BA}$, resource use of fossils: 7 $\%_{BA}$, see Figure 4) predominantly derives from dolomite production through its transportation and electricity demand, albeit from different electricity sources for different impact categories. The precious metal catalyst impact stems from the primary rhodium mining, which has its largest impact on freshwater ecotoxicity (14.2 $\%_{BA}$, Figure 4 and 11.5 $\%_{EA}$, Figure 5). Due to mostly small variations in contribution between the different cases, only case 1.4 is illustrated here. The other cases can be found in the Supplementary Information (SI Figures 1-8).

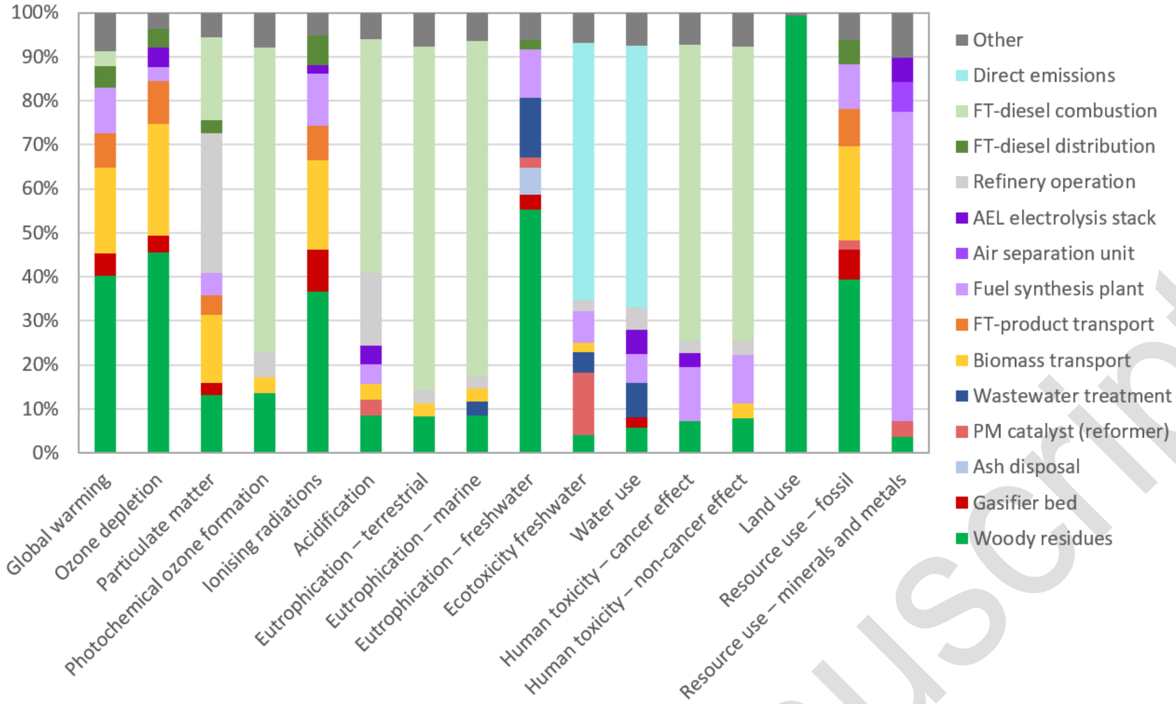

Figure 4: Impact contributions for all 16 impact categories in the BA mode for case 1.4.

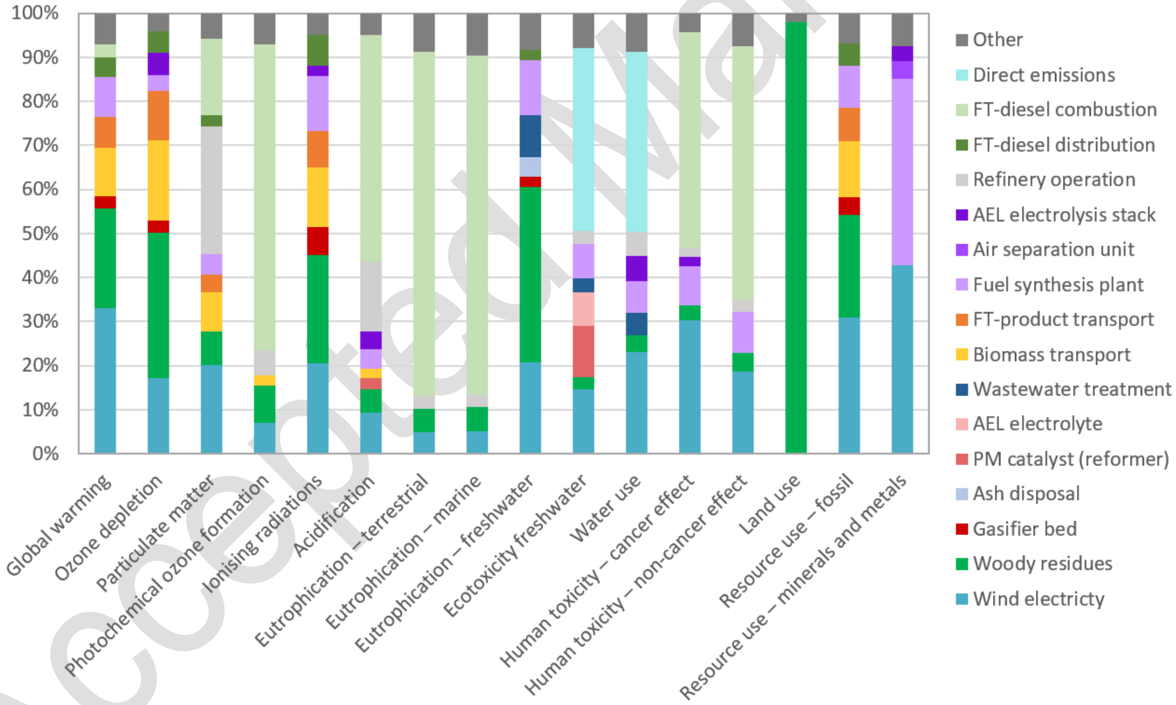

Figure 5: Impact contributions for all 16 impact categories in the EA mode for case 1.4.

3.2 Lowest impact cases

Depending on the process mode and allocation method, sets of process parameters yielding high carbon, process or fuel efficiency have the lowest environmental impacts. Table 7 summarises the cases with the lowest impact for each impact category and mode when applying energetic and economic allocation. The detailed results can be found in the Supplementary Information (SI Table 23). In total, case 1.4 (low H_2/CO ratio and low H_2 conversion) has the highest number of lowest impacts followed by case 1.3 (low H_2/CO ratio and high H_2 conversion). A low H_2/CO ratio as in case 1.3 and 1.4 enhances the product output per energetic input because less carbon is lost as CO_2 (BA mode) or less hydrogen needs to be produced (EA mode) in order to adjust the H_2/CO ratio (see 2.3). With a higher product output to input ratio, the environmental impacts are divided by a larger product amount resulting in lower impacts per MJ FT-diesel.

The distinction between case 1.4 and 1.3 lies in the different H_2 conversions. A higher H_2 conversion increases the FT-product yield due to a higher selectivity towards C_{5+} and a higher CO conversion (see 2.3). Therefore, a higher H_2 conversion and lower H_2/CO ratio (case 1.3) results in the highest fuel efficiency. When the H_2 conversion is decreased and the H_2/CO ratio stays low (case 1.4), the product output is shifted towards heat and electricity resulting in the highest process efficiency [13].

Table 7: Cases with lowest impact per impact category, mode and allocation method.

Case	BA		EA	
	energetic	economic	energetic	economic
Global warming	1.4	1.3	1.4	1.3
Ozone depletion	1.4	1.3	1.6	1.5
Particulate matter	1.4	1.4	1.4	1.3
Photochemical ozone formation	1.4	1.4	1.4	1.4
Ionising radiation	1.4	1.3	1.2	1.3
Acidification	1.4	1.4	1.4	1.4
Eutrophication – terrestrial	1.4	1.4	1.4	1.4
Eutrophication – marine	1.4	1.4	1.4	1.4
Eutrophication – freshwater	1.4	1.3	1.6	1.5
Ecotoxicity freshwater	1.4	1.3	1.6	1.5
Water use	1.4	1.3	1.4	1.3
Human toxicity – cancer effect	1.4	1.4	1.4	1.3
Human toxicity – non-cancer effect	1.4	1.4	1.4	1.4
Land use	1.4	1.3	1.6	1.6
Resource use – fossil	1.4	1.3	1.4	1.3
Resource use – minerals and metals	1.4	1.4	1.4	1.3

In the case of energetic allocation, lower impact generally correlates with higher process efficiency (case 1.4). If a larger share is allocated towards FT-diesel with economic allocation (~90 % with economic allocation vs. ~70-75 % with energetic allocation), the correlation shifts towards high fuel efficiency (case 1.3). The exception are categories where a large share of impact stems from fuel synthesis plant construction or fuel related sources (e.g., FT-diesel combustion, FT-diesel distribution, refinery operation). Since these impacts are not affected by process parameter variations, a higher fuel efficiency at the expense of overall product output (process efficiency) is not beneficial. In these categories case 1.4 has the lowest impact in both energetic and economic allocation.

In EA mode, categories with large impact contribution related to biomass and a comparatively low impact contribution from electricity result in other cases with the lowest impact. Biomass related impacts comprise woody residue production, biomass transport and direct emissions, which correlate with biomass consumption. Naturally, biomass related impacts are lowest for cases with high carbon efficiency (case 1.5 and 1.6). Case 1.6, with the maximum CO_2 recycle rate, has the highest carbon efficiency and lowest impacts with energetic allocation. Case 1.5 has the second highest carbon efficiency (CO_2 recycle rate between case 1.6 and the other cases) but a higher fuel and process efficiency than case 1.6. As there is a trade-off between reduced biomass supply and increased electricity demand with large CO_2 recycles, a higher fuel/process efficiency is beneficial when a larger portion is allocated towards FT-diesel (economic allocation). Land use, which is almost entirely caused by the biomass, has no such trade-off and hence its lowest impact at the highest carbon efficiency (case 1.6) for both allocation methods.

The same trade-off between biomass supply and electricity demand is responsible for the lowest impact of case 1.2 in the category ionising radiation (energetic allocation). Case 1.2 (high H_2/CO ratio and low H_2 conversion) has a lower process efficiency than case 1.4 (low H_2/CO ratio and low H_2 conversion) but a higher carbon efficiency because the FT-product yield increases with a constant H_2 conversion and increased H_2/CO ratio.

3.3 Environmental impacts of green FT-diesel compared with fossil diesel

The environmental impacts of the green FT-diesel are compared with fossil diesel to examine potential trade-offs in other impact categories when switching to the renewable alternative. Figure 6 shows the environmental impacts normalised to fossil diesel for BA and EA mode of case 1.4 (energetic allocation). The comparison with fossil diesel indicates an impact reduction in 11 (BA) or 10 (EA) out of 16 categories. With economic allocation the green FT-diesel has a reduction potential in 9 of 16 categories as both human toxicity categories then have an impact increase compared with fossil diesel.

Furthermore, BA has lower impacts than EA in 7 categories, higher in 5 and approximately equal in 4 categories. The results for the other cases are similar in terms of impact reduction/increase and can be found in the Supplementary Information (SI Table 24).

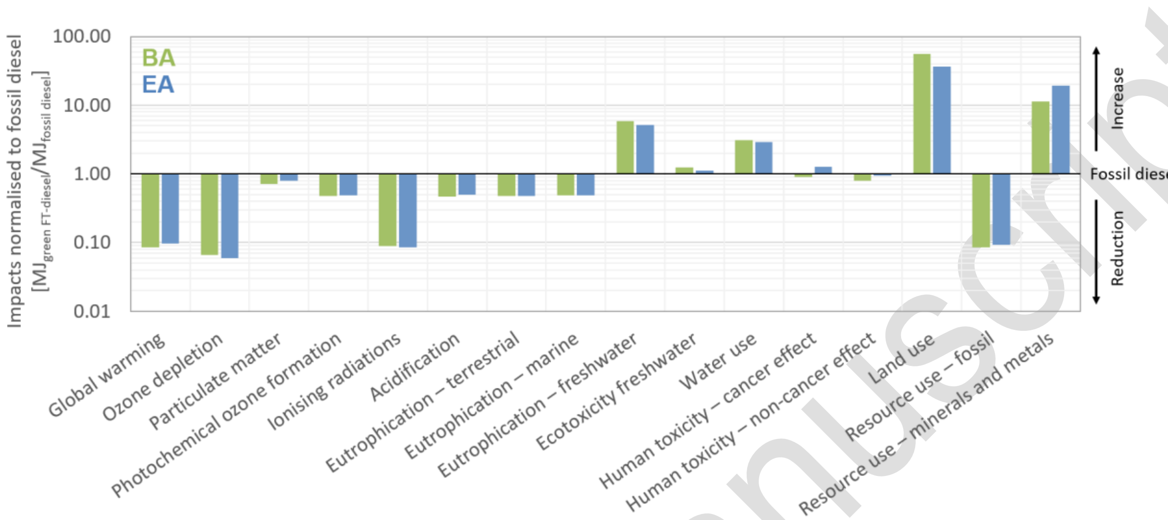

Figure 6: Environmental impact of the green FT-diesel in comparison with fossil diesel for BA and EA mode in case 1.4 (energetic allocation).

The biggest impact sources for the categories with significantly higher impacts than fossil diesel are discussed in more detail (see Figure 4 and Figure 5 for impact contributions). The sources for freshwater eutrophication impact are amongst others: wastewater of vegetable oil refining needed for sawing and harvesting (biomass); spoil treatment from lignite mining for electricity, sulfidic tailings treatment from gold and copper mine operation and spoil treatment from coal mining upstream of steel production (fuel synthesis plant); spoil treatment from coal mining upstream of steel production and sulfidic tailings treatment from copper mine operation (wind electricity). Water use is mostly generated by biomass extraction from forest and vegetable oil plant cultivation for sawing and harvesting (biomass) along with steel and nylon production (wind electricity). Land use is dominated by the biomass growth in the forest. Resource use of minerals and metals is for the most part due to copper use in construction and gold for electronics (fuel synthesis plant) as well as copper in turbine construction (wind electricity).

Land and water use were expected to be higher for a biomass based alternative fuel since there are not many origins of water use in crude oil extraction and refining and the land use for extraction and refining is also minimal. Instead of comparing these categories with fossil diesel it would be more sensible to compare different biomass sources with each other and to consider local conditions that might cause an increased impact to outweigh the reduction in global warming potential.

3.4 Sensitivity study of the global warming potential

In order to assess the influence of input parameters on the green FT-diesel GWP, input parameters with high individual contribution and high variability were varied. Figure 7 shows the effect of varying the individual GWPs of biomass (green), biomass transport (yellow) and electricity (blue) in the range from zero GWP (-100 %) to double and triple (+100 %, +200 %) the GWP of the base case. The base case (case 1.4, energetic alloc.) is indicated by a star for each mode and has the following individual impacts from biomass, biomass transport, and electricity: 3.86, 1.87, 0 $g_{CO2\text{-}eq.}/MJ_{green\ FT\text{-}diesel}$ (BA) and 2.23, 1.08, 4.09 $g_{CO2\text{-}eq.}/MJ_{green\ FT\text{-}diesel}$ (EA).

Naturally, the effect of biomass and biomass transport is larger on BA mode as more biomass is needed for the same output compared to EA mode. If the individual GWP of biomass (0.02 $kg_{CO2\text{-}eq.}/kg$) is almost doubled compared to the base case, the turning point is reached above which EA has a lower GWP than BA (①, intersection of green lines). This could be the case if another biomass source is used that is not a residue but needs to be cultivated, e.g., perennial [75] or food crops [76]. The transport GWP increases when biomass needs to be transported for more than the assumed 100 km, which can lead to EA mode becoming more favourable. The transport distance would need to be close to tripled to reach this turning point (②, intersection of yellow lines).

With regards to the turning point associated with the individual electricity GWP (③), the GWP of the blue line (EA mode) needs to be compared with the one from the base case star of BA mode. The GWP of the required energy in EA mode would have to be about 40 % lower (~10.9 $g_{CO2\text{-}eq.}/kWh$) than that of Finnish wind electricity in order for EA to have a lower GWP than BA. For example, Finnish hydro power [77] has a 77 % lower GWP, while the GWP of Finnish solar power [78] is more than 4 times higher (~320 % increase). The GWP of Finnish grid mix electricity is in between wind and solar power with 64 $g_{CO2\text{-}eq.}/kWh$ (~250 % increase) [79].

Overall, the GWP depends more on input than process parameter variations. The latter are indicated by the whiskers on the stars which represent the minimal and maximal GWP of all cases for each mode. This finding can be transferred to all other impact categories since the impact deviations between cases are small there as well.

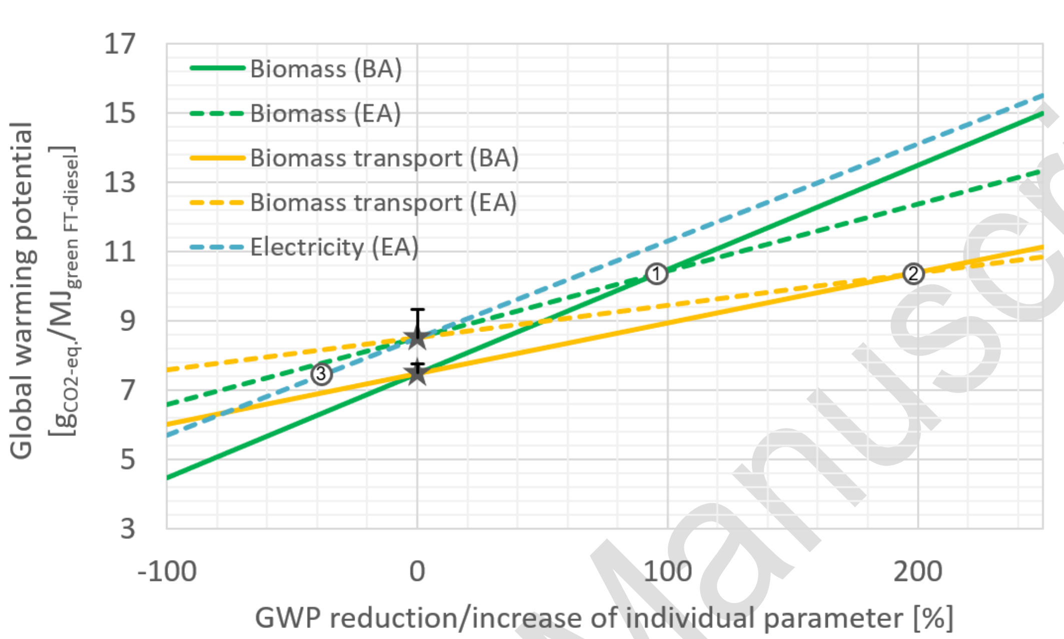

Figure 7: Sensitivity of the global warming potential (GWP) to changes in individual biomass, biomass transport and electricity GWP for case 1.4 (energetic allocation). Stars: base case GWP of case 1.4 (BA and EA) with minimum and maximum GWP (whiskers) from the other cases. Turning points of lowest green FT-diesel GWP between BA and EA mode in dependence of individual input parameters: ① – Biomass GWP turning point, ② – Biomass transport GWP turning point, ③ – Electricity GWP turning point.

3.5 Combined TEA and LCA

Table 8 shows the overall weighted impacts of this study's alternative fuel in relation to fossil diesel (WR_{AF}/WR_{FF}) for the different sets of process parameters, modes and allocation methods. The smaller the number, the lower the overall impact. A number below one signifies a lower overall impact than fossil diesel. Deviations between the cases are in the range of $2\ \%_{\text{EA, energetic alloc.}}$ to $5\ \%_{\text{BA, economic alloc.}}$. It can be concluded that a high fuel efficiency (case 1.3) is essential to achieve an overall low impact with economic allocation for both BA and EA mode. For energetic allocation low overall impact correlates with high process efficiency (case 1.4) in BA mode and high process as well as carbon efficiency (case 1.2) in EA mode.

Table 8: Weighted results ratio WR_{AF}/WR_{FF} for the six cases in BA and EA mode with energetic and economic allocation. Bold values have the lowest impact per mode and allocation method.

Allocation	Case					
	1.1	1.2	1.3	1.4	1.5	1.6
BA						
energetic	0.471	0.461	0.469	**0.457**	0.472	0.474
economic	0.568	0.575	**0.557**	0.564	0.573	0.586
EA						
energetic	0.451	**0.442**	0.452	0.443	0.449	0.446
economic	0.539	0.544	**0.536**	0.541	0.539	0.551

LCA with economic allocation yields the lowest overall impact with the case that also has the lowest NPC (see Table 2). With energetic allocation, the case with the second lowest NPC (case 1.4) has the lowest overall impact in BA mode. Case 1.2, which has the lowest overall impact in EA mode with energetic allocation, is actually the case with the second highest NPC.

Table 9 displays the cost-impact factor calculated according to Equation (2.8) and Table 10 the GHG abatement cost according to Equation (2.9). The lower the values, the lower the combined economic and ecological impact. Although differences in impact can be identified between the cases, these differences are small compared with input parameter variations. The latter is described in detail in 3.4 for the GWP. Therefore, the cost-impact factor and the greenhouse gas abatement cost are lowest for the case with the smallest NPC as the NPC is affected more by process parameter variations.

Table 9: Dimensionless cost-impact factor for the six cases in BA and EA mode with energetic and economic allocation. Bold values have the lowest factor per mode and allocation method.

Allocation	Case					
	1.1	1.2	1.3	1.4	1.5	1.6
BA						
energetic	1.15	1.18	**1.05**	1.07	1.22	1.50
economic	1.39	1.47	**1.24**	1.32	1.49	1.85
EA						
energetic	1.06	1.07	**1.01**	1.01	1.09	1.22
economic	1.27	1.32	**1.19**	1.24	1.30	1.50

Table 10: GHG abatement cost in €$_{2019}$/t$_{CO2\text{-}eq.}$ for the six cases in BA and EA mode with energetic and economic allocation. Bold values have the lowest abatement cost per mode and allocation method.

Allocation	Case					
	1.1	1.2	1.3	1.4	1.5	1.6
BA						
energetic	255.05	273.92	**217.15**	236.05	282.19	383.03
economic	259.82	279.94	**220.82**	240.88	287.67	391.32
EA						
energetic	242.84	254.28	**219.66**	230.13	254.88	311.42
economic	247.91	260.41	**223.87**	235.32	260.37	319.73

4 Conclusion

In this study, a life cycle assessment (LCA) was conducted for process parameter variations in a BtL process with flexible hydrogen addition from renewable electricity. Furthermore, a combined techno-economic and ecological assessment was performed enhancing the techno-economic results from a previous publication by Habermeyer et al. [13]. The combined techno-economic and ecological assessment in one tool has the following benefits:

- consistent functional unit and system boundaries
- development of an optimised fuel production process based on TEA and LCA
- quantification of trade-offs

The biggest environmental impact contributors of the 2nd generation biofuels process (FLEXCHX) are: biomass supply including transportation, electricity generation, fuel synthesis plant construction, green FT-diesel combustion and direct emissions (hydrogen sulphide, water). Impact from woody residues itself is primarily related to harvesting machinery operated with fossil diesel and land occupation from the growing phase. Transportation causes most of its impact through road construction, diesel and lorry production, combustion emissions as well as tyre, brake, and road wear. For wind electricity generation the construction materials of wind turbines have a significant contribution while the impact from the fuel synthesis plant construction is mainly attributed to electricity consumption, electronics and various metals. Finally, during FT-diesel combustion nitrogen oxides, dinitrogen oxide, formaldehyde and acrolein are emitted, which have a negative impact on the environment.

Green FT-diesel has lower impacts than fossil diesel in nine categories, is approximately the same in three and worse in four categories (freshwater eutrophication, water use, land use and resource use of minerals and metals). The higher impact for water use and land use is expected as origins for both are minimal in crude oil extraction and refining. Therefore, comparing different biomass sources and considering local conditions, that might cause an increased impact to outweigh the reduction in GWP, would be more sensible for these categories.

The process parameter variations demonstrated that sets of process parameters yielding high process or fuel efficiencies are favourable for nearly all impact categories. Depending on the allocation method (energetic or economic) either process or fuel efficiency corresponds with the lowest impact. However, when biomass supply is a large impact contributor, the environmental impact is lowest for sets of process parameters resulting in high carbon efficiencies. Overall, environmental impacts have a strong correlation with net production cost (NPC) when the impacts are economically allocated. Energetic allocation has no such correlation with NPC but only with technical performance parameters (process and carbon efficiency). Both the cost-impact factor and GHG abatement cost are minimised for the set of process parameters that yields the lowest NPC because environmental impacts are comparably less affected by the process parameter variations in this study. Further sensitivity studies for the GWP revealed that the operating conditions for the investigated process parameters have an overall lower effect on environmental impacts than changes in input parameters (e.g., biomass source, transport distance, electricity source).

To further reduce the global warming potential and maximise the biogenic carbon exploitation, carbon capture and storage or utilisation should be considered for the removed CO_2. As the fuel synthesis plant construction has a significant impact on multiple impact categories, the construction of each unit should be examined in more detail instead of a generic dataset. Furthermore, the conclusions drawn for the techno-economic and ecological assessment of process parameter variations should be verified for changes in process configuration (same processing route but varying individual processing steps). Different process configurations potentially entail bigger differences in technical efficiencies, environmental impacts and costs than individual process parameter variations.

Author contributions

Julia Weyand: Conceptualisation, Methodology, Software, Investigation, Formal analysis – LCA, Data curation – LCA, Validation, Writing – original draft, review & editing, Visualisation. **Felix Habermeyer**: Formal analysis – TEA, Data curation – TEA, Writing – review & editing. **Ralph-Uwe Dietrich**: Resources, Writing – review & editing, Funding acquisition, Supervision.

Declaration of competing interest

The authors declare that they have no known competing financial interests or personal relationships that could have appeared to influence the work reported in this paper.

Funding/Acknowledgement

This study is part of the FLEXCHX project, which has received funding from the European Union's Horizon 2020 research and innovation Programme under Grant Agreement No 763919.

References

[1] European Commission (2021): *'Fit for 55': delivering the EU's 2030 Climate Target on the way to climate neutrality*. Communication from the commission to the european parliament, the council, the european economic and social committee and the committee of the region. Retrieved from https://eur-lex.europa.eu/legal-content/EN/TXT/?uri=CELEX:52021DC0550.

[2] Ramsebner J., Haas R., Ajanovic A., Wietschel M. (2021): *The sector coupling concept: A critical review.* WIREs Energy and Environment, 10 (4): e396. doi: 10.1002/wene.396.

[3] Mathiesen B.V., Lund H., Connolly D., Wenzel H., Østergaard P.A., Möller B., Nielsen S., Ridjan I., Karnøe P., Sperling K., Hvelplund F.K. (2015): *Smart Energy Systems for coherent 100% renewable energy and transport solutions.* Applied Energy, 145: 139-154. doi: 10.1016/j.apenergy.2015.01.075.

[4] Blanco H., Faaij A. (2018): *A review at the role of storage in energy systems with a focus on Power to Gas and long-term storage.* Renewable and Sustainable Energy Reviews, 81: 1049-1086. doi: 10.1016/j.rser.2017.07.062.

[5] Kurkela E., Kurkela M., Frilund C., Hiltunen I., Rollins B., Steele A. (2021): *Flexible Hybrid Process for Combined Production of Heat, Power and Renewable Feedstock for Refineries : Managing seasonal energy supply and demand for heat and power in Europe.* Johnson Matthey Technology Review, 65 (2): 333-345. doi: 10.1595/205651321x16013744201583.

[6] Mahmud R., Moni S.M., High K., Carbajales-Dale M. (2021): *Integration of techno-economic analysis and life cycle assessment for sustainable process design – A review.* Journal of Cleaner Production, 317. doi: 10.1016/j.jclepro.2021.128247.

[7] Wunderlich J., Armstrong K., Buchner G.A., Styring P., Schomäcker R. (2021): *Integration of techno-economic and life cycle assessment: Defining and applying integration types for chemical technology development.* Journal of Cleaner Production, 287. doi: 10.1016/j.jclepro.2020.125021.

[8] AlNouss A., McKay G., Al-Ansari T. (2020): *A comparison of steam and oxygen fed biomass gasification through a techno-economic-environmental study.* Energy Conversion and Management, 208. doi: 10.1016/j.enconman.2020.112612.

[9] Albrecht F.G., Nguyen T.-V. (2020): *Prospects of electrofuels to defossilize transportation in Denmark – A techno-economic and ecological analysis.* Energy, 192. doi: 10.1016/j.energy.2019.116511.

[10] Isaacs S.A., Staples M.D., Allroggen F., Mallapragada D.S., Falter C.P., Barrett S.R.H. (2021): *Environmental and Economic Performance of Hybrid Power-to-Liquid and Biomass-to-Liquid Fuel Production in the United States.* Environmental Science and Technology, 55 (12): 8247-8257. doi: 10.1021/acs.est.0c07674.

[11] Albrecht F.G., König D.H., Baucks N., Dietrich R.-U. (2017): *A standardized methodology for the techno-economic evaluation of alternative fuels – A case study.* Fuel, 194: 511-526. doi: 10.1016/j.fuel.2016.12.003.

[12] Maier S., Tuomi S., Kihlman J., Kurkela E., Dietrich R.-U. (2021): *Techno-economically-driven identification of ideal plant configurations for a new biomass-to-liquid process – A case study for Central-Europe.* Energy Conversion and Management, 247. doi: 10.1016/j.enconman.2021.114651.

[13] Habermeyer F., Kurkela E., Maier S., Dietrich R.-U. (2021): *Techno-Economic Analysis of a Flexible Process Concept for the Production of Transport Fuels and Heat from Biomass and Renewable Electricity.* Frontiers in Energy Research, 9. doi: 10.3389/fenrg.2021.723774.

[14] Mutel C. (2017): *Brightway: An open source framework for Life Cycle Assessment.* Journal of Open Source Software, 2 (12): 236. doi: 10.21105/joss.00236.

[15] Wernet G., Bauer C., Steubing B., Reinhard J., Moreno-Ruiz E., Weidema B. (2016): *The ecoinvent database version 3 (part I): overview and methodology.* The International Journal of Life Cycle Assessment, 21 (9): 1218–1230. doi: 10.1007/s11367-016-1087-8.

[16] Kurkela E., Kurkela M., Hiltunen I. (2016): *Steam–oxygen gasification of forest residues and bark followed by hot gas filtration and catalytic reforming of tars: Results of an extended time test.* Fuel Processing Technology, 141: 148-158. doi: 10.1016/j.fuproc.2015.06.005.

[17] Hannula I. (2016): *Hydrogen enhancement potential of synthetic biofuels manufacture in the European context: A techno-economic assessment.* Energy, 104: 199-212. doi: 10.1016/j.energy.2016.03.119.

[18] Hillestad M., Ostadi M., Alamo Serrano G.d., Rytter E., Austbø B., Pharoah J.G., Burheim O.S. (2018): *Improving carbon efficiency and profitability of the biomass to liquid process with hydrogen from renewable power.* Fuel, 234: 1431-1451. doi: 10.1016/j.fuel.2018.08.004.

[19] Kurkela E., Kurkela M., Hiltunen I. (2014): *The effects of wood particle size and different process variables on the performance of steam-oxygen blown circulating fluidized-bed gasifier.* Environmental Progress & Sustainable Energy, 33 (3): 681-687. doi: 10.1002/ep.12003.

[20] Larsson A.-C. (2017): *Study of Catalyst Deactivation in Three Different Industrial Processes.* (Doctoral thesis). Växjö University.

[21] Toppinen S., Eilos I., Simell P., Kurkela E., Hiltunen I. (2013): *Method of Reforming Gasification Gas.* United States. Patent No. US 2013/0058855 A1. NESTE OIL OYJ, Espoo (FI). Retrieved from https://patents.google.com/patent/US20130058855A1/en.

[22] Amjad U.-E.S., Vita A., Galletti C., Pino L., Specchia S. (2013): *Comparative Study on Steam and Oxidative Steam Reforming of Methane with Noble Metal Catalysts.* Industrial & Engineering Chemistry Research, 52 (44): 15428-15436. doi: 10.1021/ie400679h.

[23] Gerber M.A. (2007): *Review of Novel Catalysts for Biomass Tar Cracking and Methane Reforming*. PNNL-16950. Pacific Northwest National Laboratory.

[24] Jones G., Jakobsen J., Shim S., Kleis J., Andersson M., Rossmeisl J., Abildpedersen F., Bligaard T., Helveg S., Hinnemann B. (2008): *First principles calculations and experimental insight into methane steam reforming over transition metal catalysts.* Journal of Catalysis, 259 (1): 147-160. doi: 10.1016/j.jcat.2008.08.003.

[25] Santos D.C.R.M., Lisboa J.S., Passos F.B., Noronha F.B. (2004): *Characterization of steam-reforming catalysts.* Brazilian Journal of Chemical Engineering, 21 (2): 203-209. doi: 10.1590/S0104-66322004000200009.

[26] Sehested J., Gelten J.A.P., Remediakis I.N., Bengaard H., Nørskov J.K. (2004): *Sintering of nickel steam-reforming catalysts: effects of temperature and steam and hydrogen pressures.* Journal of Catalysis, 223 (2): 432-443. doi: 10.1016/j.jcat.2004.01.026.

[27] Oliveira E.L.G., Grande C.A., Rodrigues A.r.E. (2009): *Steam methane reforming in a Ni/Al2O3catalyst: Kinetics and diffusional limitations in extrudates.* The Canadian Journal of Chemical Engineering, 87 (6): 945-956. doi: 10.1002/cjce.20223.

[28] Liu B., Zhao L., Wu Z., Zhang J., Zong Q., Almegren H., Wei F., Zhang X., Zhao Z., Gao J., Xiao T. (2019): *Recent Advances in Industrial Sulfur Tolerant Water Gas Shift Catalysts for Syngas Hydrogen Enrichment: Application of Lean (Low) Steam/Gas Ratio.* Catalysts, 9 (9): 772. doi: 10.3390/catal9090772.

[29] Nikolova D., Edreva-Kardjieva R., Kolev H., Gabrovska M. (2020): *Promoted Re/Al2O3 systems as sour water-gas shift catalysts.* Catalysis Today, 357: 590-601. doi: 10.1016/j.cattod.2019.05.038.

[30] Sasaki T., Suzuki T., Akasaka Y., Takaoka M. (2017): *Generation efficiency improvement of IGCC with CO 2 capture by the application of the low temperature reactive shift catalyst.* Energy, 118: 60-67. doi: 10.1016/j.energy.2016.12.023.

[31] Singh B., Strømman A.H., Hertwich E.G. (2011): *Comparative impact assessment of CCS portfolio: Life cycle perspective.* Energy Procedia, 4: 2486-2493. doi: 10.1016/j.egypro.2011.02.144.

[32] Frilund C., Simell P., Kaisalo N., Kurkela E., Koskinen-Soivi M.L. (2020): *Desulfurization of Biomass Syngas Using ZnO-Based Adsorbents: Long-Term Hydrogen Sulfide Breakthrough Experiments.* Energy and Fuels, 34 (3): 3316-3325. doi: 10.1021/acs.energyfuels.9b04276.

[33] Pearson R., Coe A., Paterson J. (2021): *Innovation in Fischer-Tropsch: A Sustainable Approach to Fuels Production : A cost-effective method of converting any carbon source into high-quality liquid hydrocarbon fuels.* Johnson Matthey Technology Review, 65 (3): 395-403. doi: 10.1595/205651321x16143384043486.

[34] Todic B., Bhatelia T., Froment G.F., Ma W., Jacobs G., Davis B.H., Bukur D.B. (2013): *Kinetic Model of Fischer–Tropsch Synthesis in a Slurry Reactor on Co–Re/Al2O3 Catalyst.* Industrial & Engineering Chemistry Research, 52 (2): 669-679. doi: 10.1021/ie3028312.

[35] Vega-Merino P., García-López A., Agueda-Rangel R., Martínez-Moreno V. (2018): *ULSD production at moderate operating pressure with a NiMo/γ-Al2O3 catalyst and a middle distillates mixture defined by sulfur distribution*. ISCRE25 - The 25th International Symposium on Chemical Reaction Engineering. Florence, Italy, 20-23 May 2018.

[36] BASF (2020): High Performance Spherical Catalysts Carriers. Retrieved from https://catalysts.basf.com/files/literature-library/Spheres_Supports_Datasheet_Updated.pdf.

[37] Griffiths D.C., Kneale B. (1992): *Catalysts.* US 005110781 A. Retrieved from https://patents.google.com/patent/US5110781.

[38] Suehiro M., Nagaki Y., Inui T., Takegami Y. (1983): *Methanol Conversion on Ni/SiO2 and Ni/Al2O3 Catalysts.* Journal of The Japan Petroleum Institute, 26 (2): 150-155. doi: 10.1627/jpi1958.26.150.

[39] Bartholomew C.H., Farrauto R.J. (2005): *Reactors, Reactor Design, and Activity Testing*, in: C.H. Bartholomew and R.J. Farrauto, (Eds.): *Fundamentals of Industrial Catalytic Processes*, John Wiley & Sons, Inc.: 197-259. ISBN 9780471730071. doi: 10.1002/9780471730071.ch4.

[40] Todic B., Ma W., Jacobs G., Davis B.H., Bukur D.B. (2014): *Effect of process conditions on the product distribution of Fischer–Tropsch synthesis over a Re-promoted cobalt-alumina catalyst using a stirred tank slurry reactor.* Journal of Catalysis, 311: 325-338. doi: 10.1016/j.jcat.2013.12.009.

[41] Rytter E., Holmen A. (2017): *Perspectives on the Effect of Water in Cobalt Fischer–Tropsch Synthesis.* ACS Catalysis, 7 (8): 5321-5328. doi: 10.1021/acscatal.7b01525.

[42] Rytter E., Holmen A. (2015): *Deactivation and Regeneration of Commercial Type Fischer-Tropsch Co-Catalysts — A Mini-Review.* Catalysts, 5 (2): 478-499. doi: 10.3390/catal5020478.

[43] Luke (2020): Growing stock volume on forest land and poorly productive forest land by tree species by inventory, region and tree species (Statistics database). Natural Resources Institute Finland (Luke). [accessed 06.07.2022]. Retrieved from https://statdb.luke.fi/PXWeb/pxweb/en/LUKE/LUKE__04%20Metsa__06%20Metsavarat/1.16_Puuston_tilavuus_metsa_ja_kitumaalla_pu.px/table/tableViewLayout2/?rxid=f8ed5f38-9607-4c55-91c9-791d660b234e.

[44] Puuinfo Ltd. (2020): *Strength properties of wood*. Why wood? Wood as a material. last updated: 29.07.2020. [accessed 11.08.2022]. Available at: https://puuinfo.fi/puutieto/wood-as-a-material/strength-properties-of-wood/?lang=en.

[45] Liepiņš J., Liepiņš K. (2015): *Evaluation of Bark Volume of Four Tree Species in Latvia*. Research for Rural Development. LLU, Jelgava.

[46] Routa J., Brännström H., Anttila P., Mäkinen M., Jänis J., Asikainen A. (2017): *Wood extractives of Finnish pine, spruce and birch – availability and optimal sources of compounds*. Natural resources and bioeconomy studies. Vol. 73. ISBN 978-952-326-495-3.

[47] Nosek R., Holubcik M., Jandacka J. (2016): *The Impact of Bark Content of Wood Biomass on Biofuel Properties.* BioResources, 11 (1): 44-53. doi: 10.15376/biores.11.1.44-53.

[48] Werner F. (2021): *softwood forestry, pine, sustainable forest management, SE, Undefined, ecoinvent database version 3.8*.

[49] Dong H., Zhao J., Chen J., Wu Y., Li B. (2015): *Recovery of platinum group metals from spent catalysts: A review.* International Journal of Mineral Processing, 145: 108-113. doi: 10.1016/j.minpro.2015.06.009.

[50] Rombach E., Friedrich B. (2014): *Recycling of Rare Metals*: *Handbook of Recycling*: 125-150. ISBN 9780123964595. doi: 10.1016/b978-0-12-396459-5.00010-6.

[51] Kloprogge J.T., Ponce C.P., Loomis T. (2020): *The Periodic Table: Nature's Building Blocks. An Introduction to the Naturally Occurring Elements, Their Origins and Their Uses*. Elsevier Science. ISBN 9780128215388.

[52] Gatti M., Martelli E., Maréchal F., Consonni S. (2015): *Multi-Objective Optimization of a Selexol®Process for the Selective Removal of CO_2 and H_2S from Coal-Derived Syngas*. ECOS 2015 - The 28th international conference on Efficiency, Cost, Optimization, Simulation and environmental impact of energy systems. France, June 30 - July 3, 2015.

[53] Mcjannett J. (2012): *Using physical solvent in multiple applications*. [accessed 14.01.2022]. Available at: https://www.digitalrefining.com/article/1000359/using-physical-solvent-in-multiple-applications.

[54] Xin K., Hashish M., Roghair I., van Sint Annaland M. (2020): *Process Simulation and Economic Analysis of Pre-combustion CO_2 Capture With Deep Eutectic Solvents.* Frontiers in Energy Research, 8. doi: 10.3389/fenrg.2020.573267.

[55] Kubek D.J., Polla E., Wilcher F.P. (2000): *Purification and Recovery Options for Gasification*. Gasification Technologies Conference. San Francisco, California, USA, October 1996. UOP.

[56] Schakel W., Meerman H., Talaei A., Ramírez A., Faaij A. (2014): *Comparative life cycle assessment of biomass co-firing plants with carbon capture and storage.* Applied Energy, 131: 441-467. doi: 10.1016/j.apenergy.2014.06.045.

[57] European Commission (2014): *Commission decision of 18 December 2014 amending Decision 2000/532/EC on the list of waste pursuant to Directive 2008/98/EC of the European Parliament and of the Council*. Official Journal of the European Union.

[58] Jungbluth N., Frischknecht R., Faist Emmenegger M., Steiner R., Tuchschmid M. (2007): *Life Cycle Assessment of BTL-fuel production: Inventory Analysis*. In: Renewable fuels for advanced powertrains (RENEW). D 5.2.7. ESU-services Ltd.

[59] Koj J., Wulf C., Schreiber A., Zapp P. (2017): *Site-Dependent Environmental Impacts of Industrial Hydrogen Production by Alkaline Water Electrolysis.* Energies, 10 (7). doi: 10.3390/en10070860.

[60] Gilani B., Stuart P.R. (2015): *Life cycle assessment of an integrated forest biorefinery: hot water extraction process case study.* Biofuels, Bioproducts and Biorefining, 9 (6): 677-695. doi: 10.1002/bbb.1570.

[61] Trzciński G., Tymendorf Ł., Kozakiewicz P. (2021): *Parameters of Trucks and Loads in the Transport of Scots Pine Wood Biomass Depending on the Season and Moisture Content of the Load.* Forests, 12 (2). doi: 10.3390/f12020223.

[62] Johnson L., Lippke B., Oneil E. (2012): *Modeling Biomass Collection and Woods Processing Life-Cycle Analysis.* Forest Products Journal, 62 (4): 258-272. doi: 10.13073/fpj-d-12-00019.1.

[63] Han J., Forman G.S., Elgowainy A., Cai H., Wang M., DiVita V.B. (2015): *A comparative assessment of resource efficiency in petroleum refining.* Fuel, 157: 292-298. doi: 10.1016/j.fuel.2015.03.038.

[64] Engineering ToolBox (2003): *Fuels - Higher and Lower Calorific Values*. [accessed 07.09.2022]. Available at: https://www.engineeringtoolbox.com/fuels-higher-calorific-values-d_169.html.

[65] Jungbluth N. (2007): *Erdöl*. In: Sachbilanzen von Energiesystemen: Grundlagen für den ökologischen Vergleich von Energiesystemen und den Einbezug von Energiesystemen in Ökobilanzen für die Schweiz (Ed. R. Dones). ecoinvent report No. 6-IV Swiss Centre for Life Cycle Inventories. Dübendorf and Villigen, CH.

[66] Lappas A., Heracleous E. (2011): *Production of biofuels via Fischer-Tropsch synthesis: biomass-to-liquids*, in: R. Luque, J. Campelo, and J. Clark, (Eds.): *Handbook of Biofuels Production*, Woodhead Publishing: 493-529. ISBN 9781845696795. doi: 10.1533/9780857090492.3.493.

[67] Fazio S., Biganzioli F., De Laurentiis V., Zampori L., Sala S., Diaconu E. (2018): *Supporting information to the characterisation factors of recommended EF Life Cycle Impact Assessment methods: Version 2 from ILCD to EF 3.0*. In: JRC Technical Reports. European Commission. Joint Research Centre. doi: 10.2760/002447.

[68] European Commission (2019): *EF 3.0 Complete pack*. Retrieved from: https://eplca.jrc.ec.europa.eu/LCDN/EF_archive.xhtml.

[69] Sala S., Cerutti A.K., Pant R. (2018): *Development of a weighting approach for the Environmental Footprint*. In: JRC Technical Reports. European Comission. Joint Research Centre. doi: 10.2760/945290.

[70] en2x (2022): *Average annual OPEC crude oil price from 1960 to 2022 (in U.S. dollars per barrel)*. [Graph]. last updated: 26.08.2022. [accessed 20.09.2022]. Available at: https://www.statista.com/statistics/262858/change-in-opec-crude-oil-prices-since-1960/.

[71] Statista (2022): *Euro (EUR) to U.S. dollar (USD) exchange rate from January 1999 to September 2, 2022*. [Graph]. last updated: 05.09.2022. [accessed 20.09.2022]. Available at: https://www.statista.com/statistics/412794/euro-to-u-s-dollar-annual-average-exchange-rate/.

[72] Engineering ToolBox (2008): *Fossil and Alternative Fuels - Energy Content*. [accessed 24.08.2022]. Available at: https://www.engineeringtoolbox.com/fossil-fuels-energy-content-d_1298.html.

[73] Neste Corporation (2020): *Financial Statements Release for 2019*. Available at: https://www.neste.com/sites/neste.com/files/release_attachments/neste_financial_statements_2019.pdf.

[74] European Parliament (2018): *Directive 2018/2001 of the European Parliament and of the Council of 11 December 2018 on the promotion of the use of energy from renewable sources (recast).* Official Journal of the European Union. Retrieved from https://eur-lex.europa.eu/legal-content/EN/TXT/PDF/?uri=CELEX:32018L2001&from=EN.

[75] Wagner M., Lewandowski I. (2017): *Relevance of environmental impact categories for perennial biomass production.* GCB Bioenergy, 9 (1): 215-228. doi: 10.1111/gcbb.12372.

[76] Nemecek T., Weiler K., Plassmann K., Schnetzer J., Gaillard G., Jefferies D., García–Suárez T., King H., Milà i Canals L. (2012): *Estimation of the variability in global warming potential of*

worldwide crop production using a modular extrapolation approach. Journal of Cleaner Production, 31: 106-117. doi: 10.1016/j.jclepro.2012.03.005.

[77] Treyer K. (2021): *electricity production, hydro, run-of-river, FI, Allocation, cut-off by classification, ecoinvent database version 3.8*.

[78] Bauer C. (2021): *electricity production, photovoltaic, 3kWp slanted-roof installation, multi-Si, panel, mounted, FI, Allocation, cut-off by classification, ecoinvent database version 3.8*.

[79] European Environment Agency (2022): *Greenhouse gas emission intensity of electricity generation in Europe*. last updated: 14.07.2022. [accessed 17.10.2022]. Available at: https://www.eea.europa.eu/ims/greenhouse-gas-emission-intensity-of-1.